

Supporting Information

Porous and Low-Crystalline Manganese Silicate Hollow Spheres Wired by Graphene Oxide for High-Performance Lithium and Sodium Storage

Jiexin Zhu,[†] Chunjuan Tang,^{*,†,‡} Zechao Zhuang,[†] Changwei Shi,[†] Narui Li,[†] Liang Zhou[†] and Liqiang Mai^{*,†,§}

[†] State Key Laboratory of Advanced Technology for Materials Synthesis and Processing, Wuhan University of Technology, Wuhan 430070, Hubei, P. R. China.

[‡] Department of Mathematics and Physics, Luoyang Institute of Science and Technology, Luoyang 471023, P. R. China.

[§] Department of Materials Science and Engineering, University of California at Los Angeles, Los Angeles, California 90095-6989, United States

E-mail: tangchunjuan@163.com; mlq518@whut.edu.cn

EXPERIMENTAL SECTION

Synthesis of MS/GO and MS/RGO

0.1 g Stöber SiO₂ spheres with a diameter of ~ 400 nm was dispersed into 18 mL deionized water by ultrasonication. 1.3 mmol MnCl₂·4H₂O, 10 mmol NH₄Cl, and 0.85 mL NH₃·H₂O were sequentially added into 20 mL deionized water under stirring. The two solutions were mixed together and stirred for another 10 min. The mixed solution was then transferred to a Teflon-lined stainless-steel autoclave and heated in an oven at 140 °C for 24 h. The resulting brown precipitate (MS) was collected by centrifugation, washed with deionized water and ethanol for three times and dried at 60 °C for 8 h.

100 mg MS was re-dispersed into 30 mL deionized water by ultrasonication. 3.5 mL GO solution (3.1 mg mL⁻¹), which was synthesized by the modified Hummer's method (graphite: KMnO₄ = 1: 1.5), was dispersed into 20 mL deionized water by ultrasonication. The two solutions were mixed, stirred for 10 h, and freeze-dried to obtain the MS/GO composite. The MS/GO composite was heated at 700 °C for 10 h under Ar containing 5% H₂ atmosphere to yield MS/reduced graphene oxide (MS/RGO).

Materials characterization

X-Ray diffraction (XRD) patterns were collected by a D8 Advance X-ray diffractometer using Cu-K α radiation ($\lambda = 1.5418 \text{ \AA}$). Thermogravimetric Analysis (TGA) was performed using a Netzsch STA 449C analyzer. Raman spectrum was obtained using a Renishaw INVIA micro-Raman spectroscopy system.

Brunauer-Emmet-Teller (BET) surface areas were measured using a Tristar II 3020 instrument by nitrogen sorption of at 77 K. The morphology and microstructure of the products were investigated with field emission scanning electron microscopy (FESEM) on a JEOL-7100F microscope, transmission electron microscopy (TEM) and high-resolution TEM (HRTEM) on a JEM-2100F microscope.

Electrochemical Characterizations

The electrochemical properties were characterized by assembling 2016-type coin cells with lithium foil as the counter electrode. The working electrodes were consisted of 70 wt% active material, 25 wt% acetylene black, and 5 wt% carboxyl methyl cellulose binder. The slurry was cast onto the copper foil and dried at 70 °C for 12 h. The mass loading of active material is 1.5 – 2 mg cm⁻². The electrolyte was composed of 1.0 M LiPF₆ in ethylene carbonate/dimethyl carbonate with a volume ratio of 1:1. The cells were aged for 4 h before electrochemical characterization to ensure full penetration of the electrolyte into the electrodes. Galvanostatic discharge/charge measurements were performed on a multichannel battery testing system (LAND CT2001A). Electrochemical performance testing at high temperature was performed in high and low temperature test chamber (KW-LH-72). Cyclic voltammetry (CV) was performed using an electrochemical workstation (CHI 760E). Electrochemical impedance spectra (EIS) were tested with an Autolab Potentiostat Galvanostat (PGSTAT302N).

ADDITIONAL FIGURES

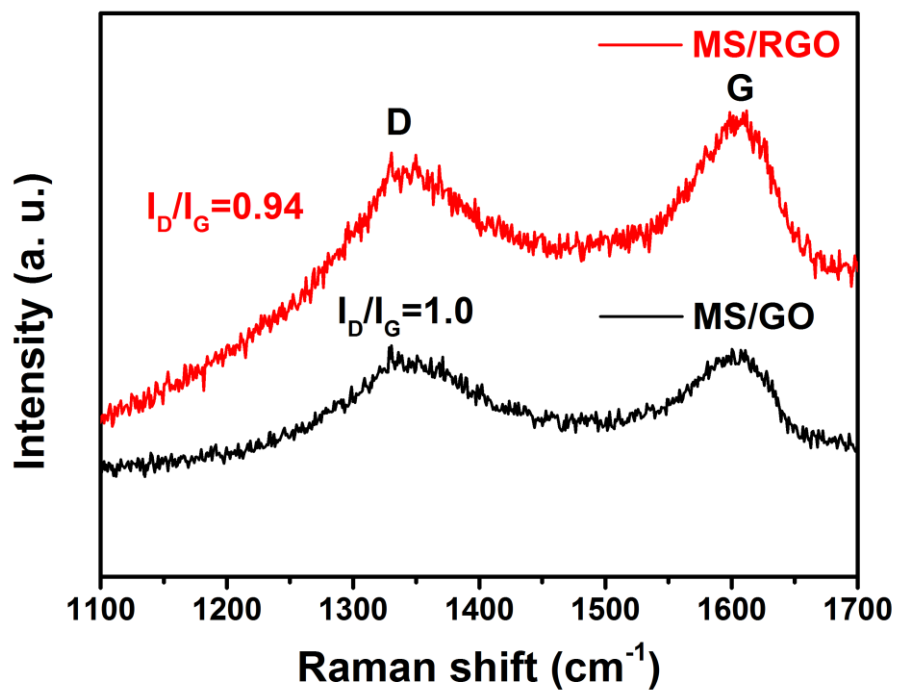


Figure S1. Raman spectrum of MS/GO and MS/RGO.

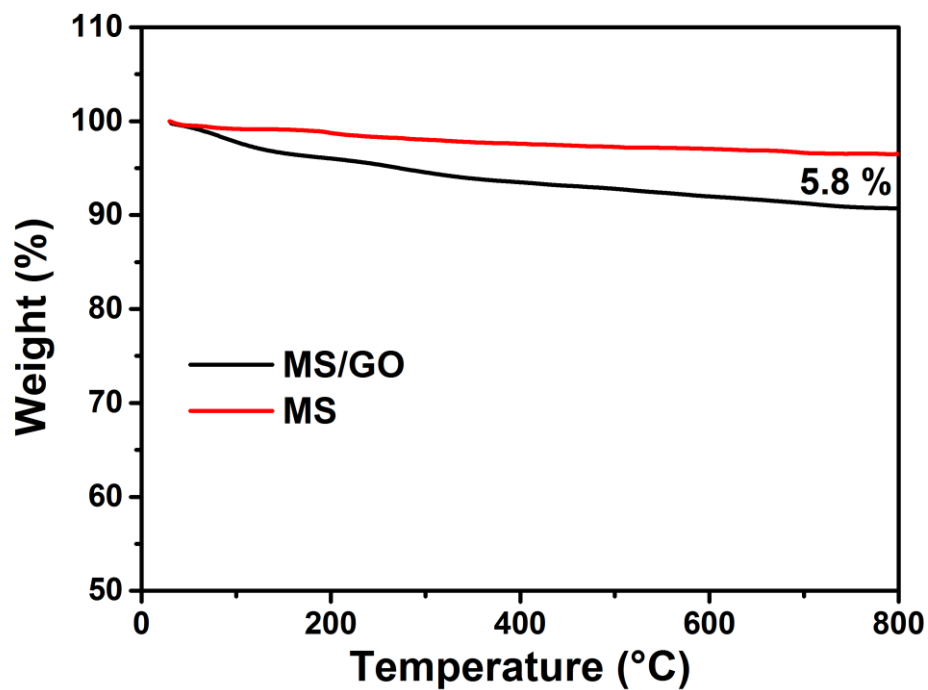


Figure S2. TGA curves of MS/GO and pure MS

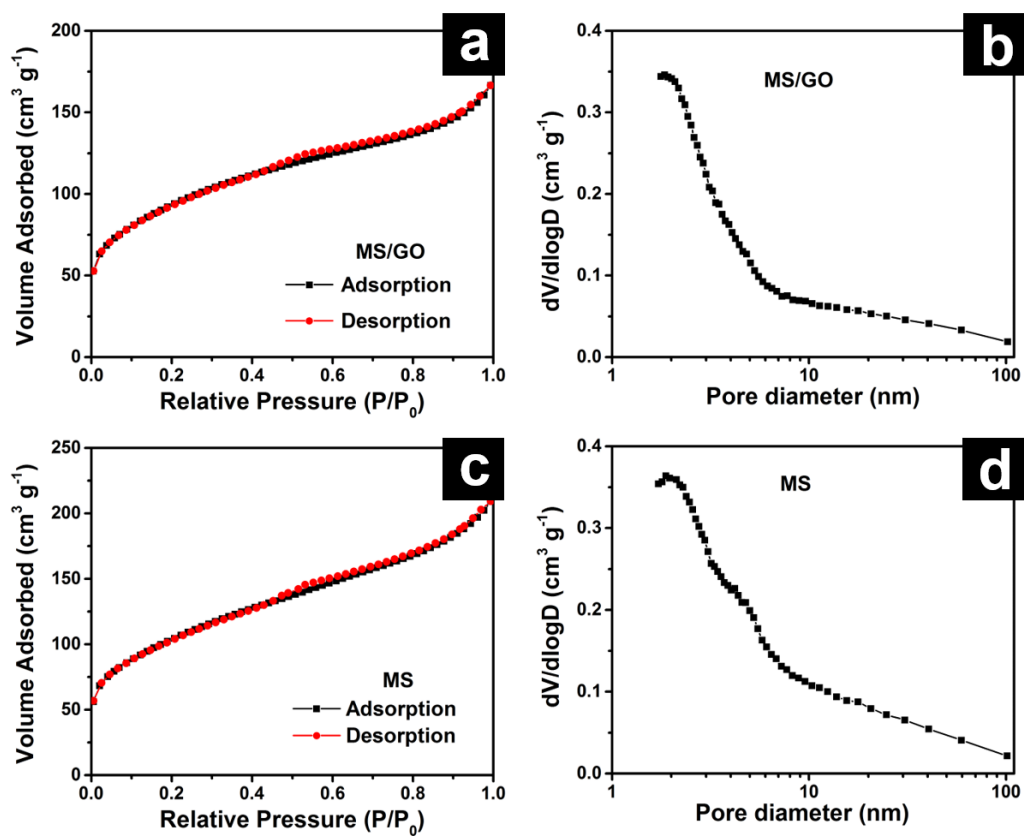


Figure S3. Nitrogen adsorption-desorption isotherms and the corresponding pore size distributions of MS/GO (a, b) and MS (c, d).

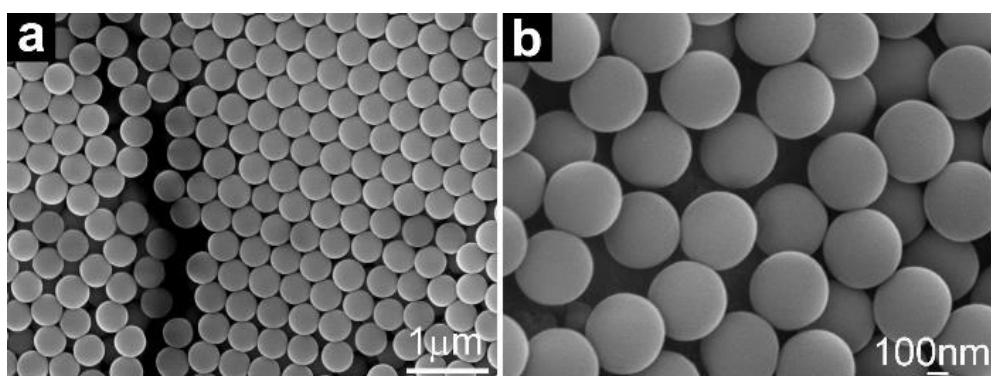


Figure S4. (a, b) SEM images of SiO_2 spheres.

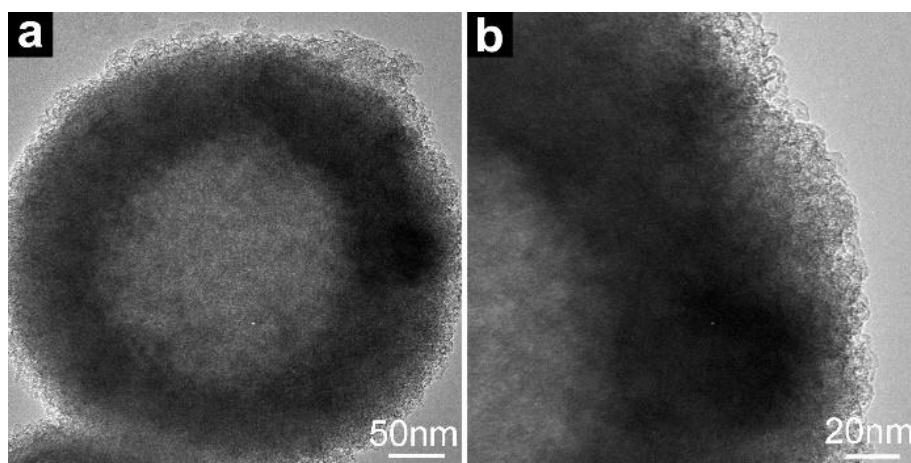


Figure S5 (a, b) TEM images of MS.

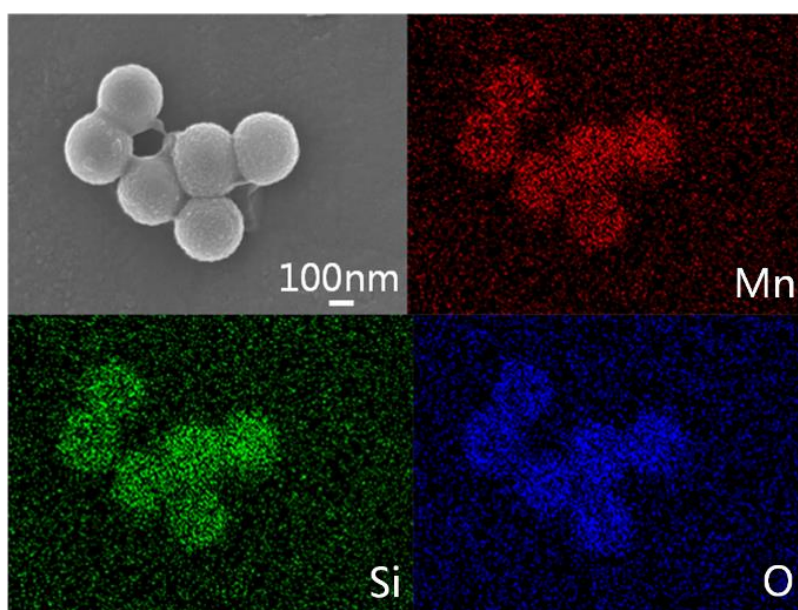


Figure S6. Elemental-mapping result of MS.

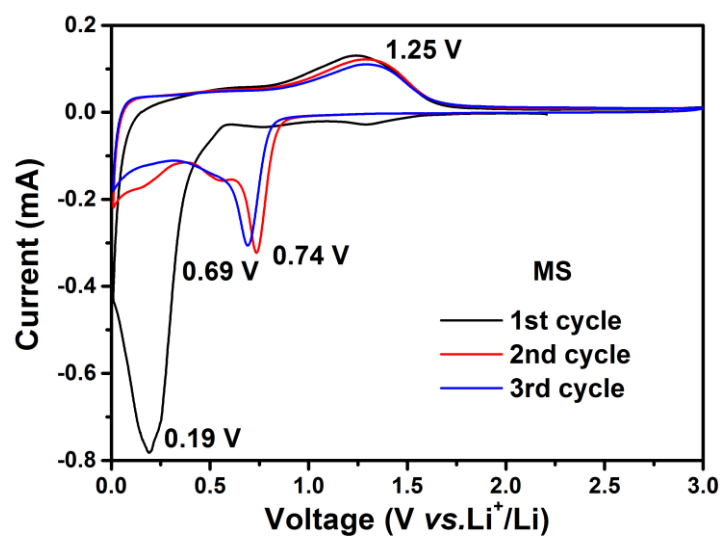


Figure S7. CV curve of MS.

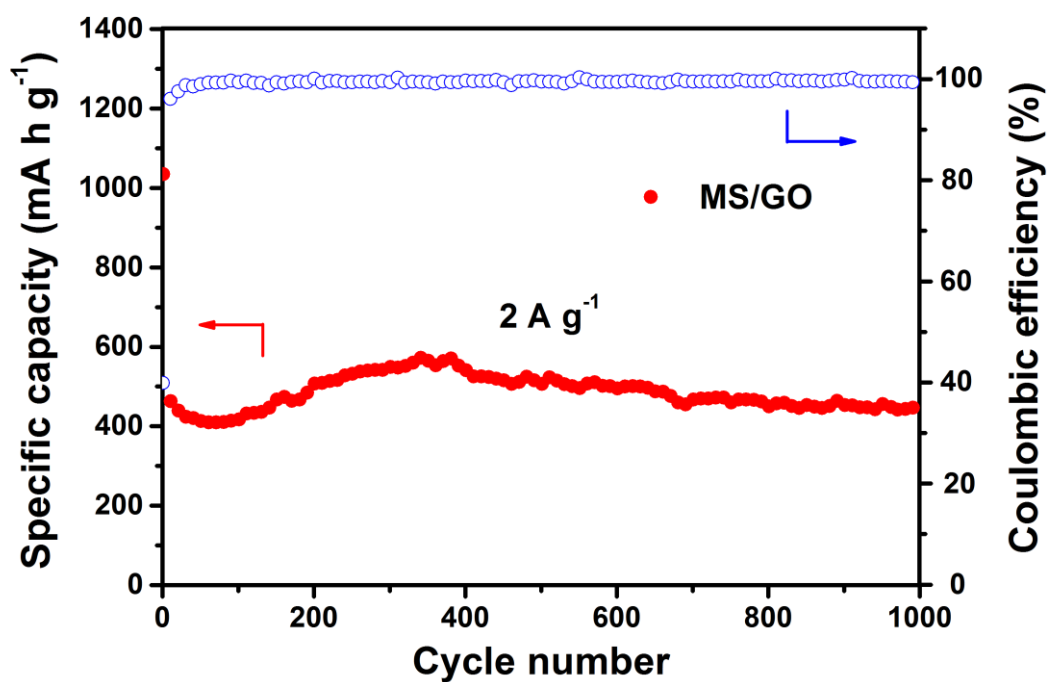


Figure S8. Cycling performance and coulombic efficiency of MS/GO at a current density of 2 A g⁻¹.

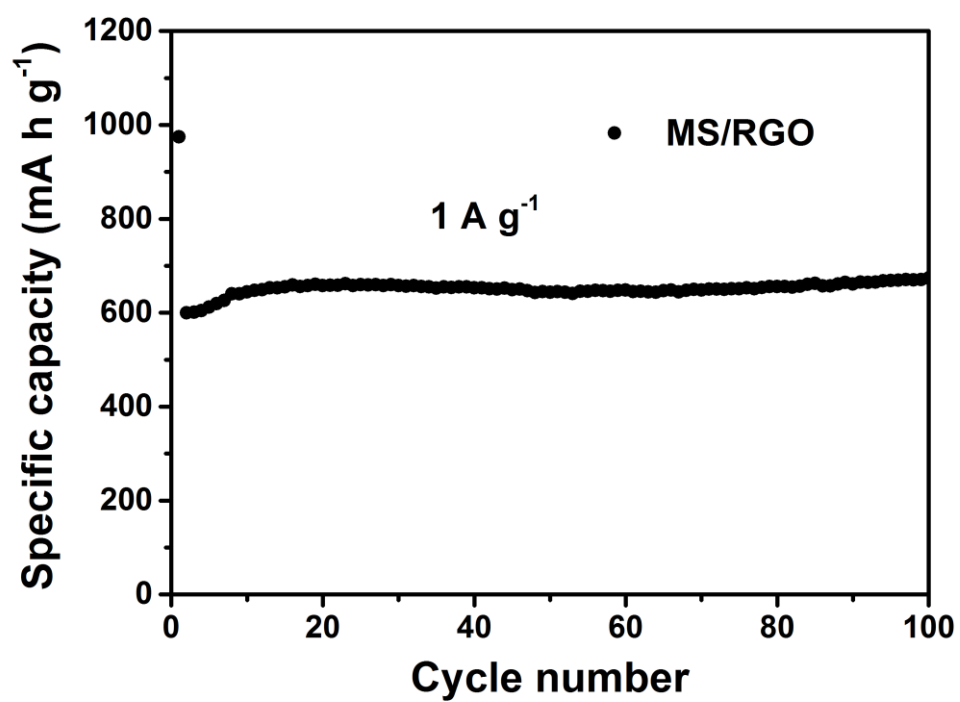


Figure S9. Cycling performance of MS/RGO at the current density of 1 A g^{-1} .

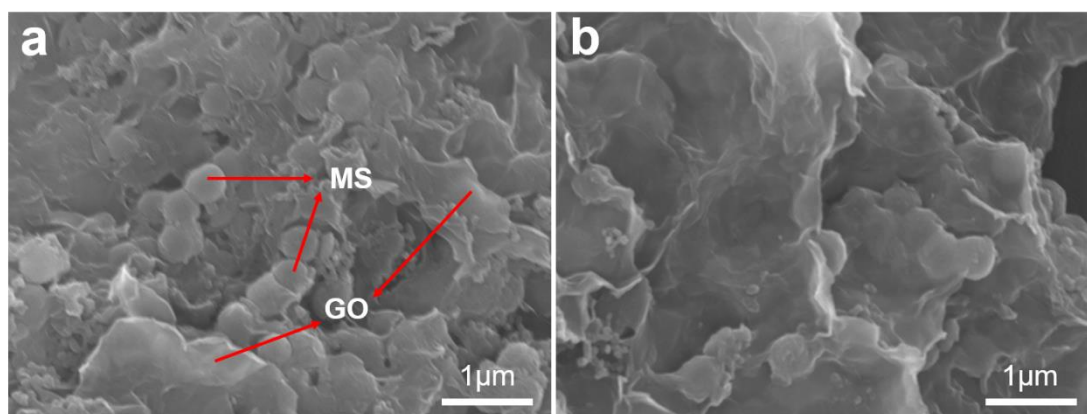


Figure S10. (a, b) SEM images of MS/GO after 500 cycles at a current density of 1 A g^{-1} .

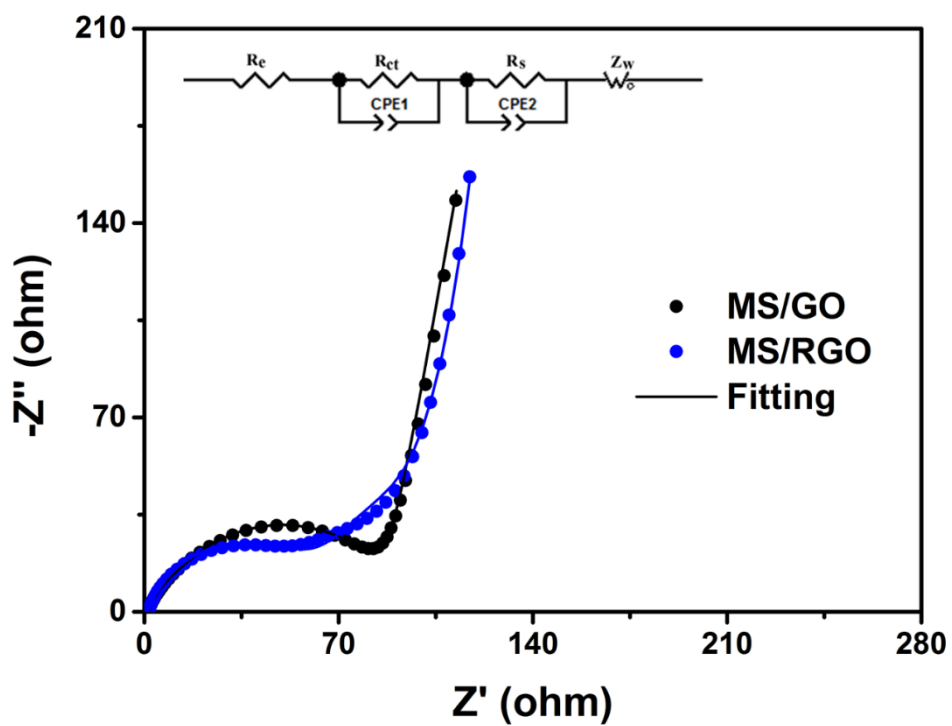


Figure S11. Nyquist plots of MS/GO and MS/RGO, R_e = external resistance, R_{ct} = charge-transfer resistance, CPE = constant phase element, R_s = SEI resistance, and Z_w = Warburg impedance.

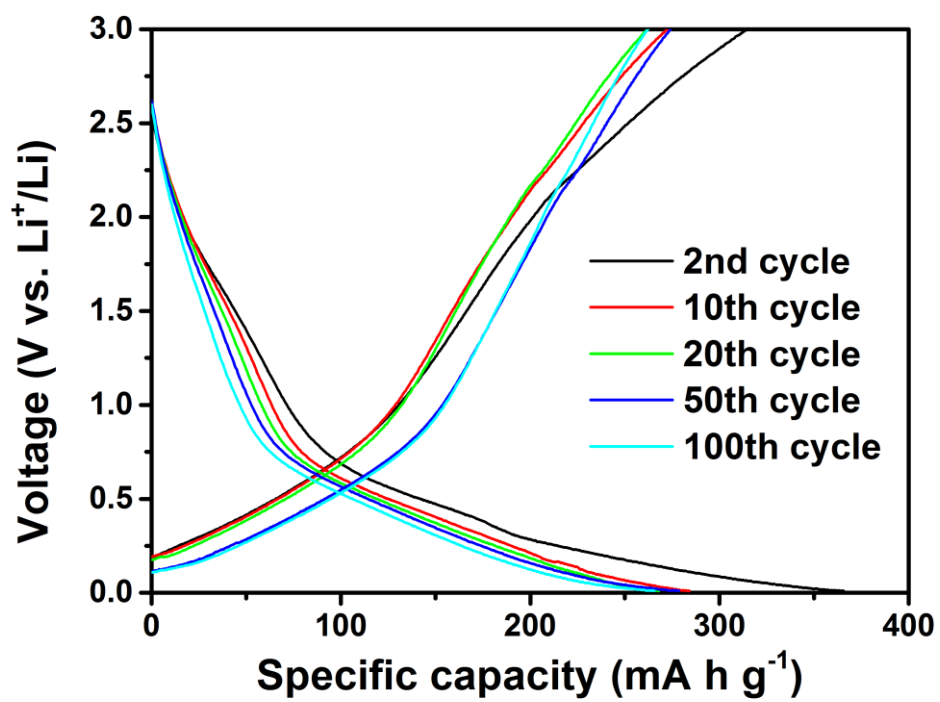


Figure S12. Discharge-charge curves of MS/GO at 0.2 A g⁻¹ for sodium storage.